Belief-propagation algorithm and the Ising model on networks with arbitrary distributions of motifs

S. Yoon,[1] A. V. Goltsev,[1,2] S. N. Dorogovtsev,[1,2] and J. F. F. Mendes[1]
[1] *Departamento de Física da Universidade de Aveiro, I3N, 3810-193 Aveiro, Portugal*
[2] *A. F. Ioffe Physico-Technical Institute, 194021 St. Petersburg, Russia*

(Dated: June 27, 2011)

We generalize the belief-propagation algorithm to sparse random networks with arbitrary distributions of motifs (triangles, loops, etc.). Each vertex in these networks belongs to a given set of motifs (generalization of the configuration model). These networks can be treated as sparse uncorrelated hypergraphs in which hyperedges represent motifs. Here a hypergraph is a generalization of a graph, where a hyperedge can connect any number of vertices. These uncorrelated hypergraphs are tree-like (hypertrees), which crucially simplify the problem and allow us to apply the belief-propagation algorithm to these loopy networks with arbitrary motifs. As natural examples, we consider motifs in the form of finite loops and cliques. We apply the belief-propagation algorithm to the ferromagnetic Ising model on the resulting random networks. We obtain an exact solution of this model on networks with finite loops or cliques as motifs. We find an exact critical temperature of the ferromagnetic phase transition and demonstrate that with increasing the clustering coefficient and the loop size, the critical temperature increases compared to ordinary tree-like complex networks. Our solution also gives the birth point of the giant connected component in these loopy networks.

PACS numbers: 05.10.-a, 05.40.-a, 05.50.+q, 87.18.Sn

I. INTRODUCTION

The belief-propagation algorithm is an effective numerical method for solving inference problems on sparse graphs. It was originally proposed by J. Pearl [1] for tree-like graphs. The belief-propagation algorithm was applied to study diverse systems in computer science, physics, and biology. Among its numerous applications are computer vision problems, decoding of high performance turbo codes and many others, see [2, 3]. Empirically, it was found that this algorithm works surprisingly good even for graphs with loops. Yedidia *et al.* [4] found that the belief-propagation algorithm actually coincides with the minimization of the Bethe free energy. This discovery renewed interest in the Bethe-Peierls approximation and related methods [5–7]. In statistical physics the belief-propagation algorithm is equivalent to the so-called *cavity method* proposed by Mézard, Parisi, and Virasoro [8]. The belief-propagation algorithm is applicable to models with both discrete and continuous variables [9–11]. Recently the belief-propagation algorithm was applied to diverse problems in random networks: the disease spreading [12], the calculation of the size of giant component [13], counting large loops in directed random uncorrelated networks [14], the graph bipartitioning problem [15], the analysis of the contributions of individual nodes and groups of nodes to the network structure [16], and networks of spiking neurons [17].

These investigations showed that the belief-propagation algorithm is exact for a model on a graph with locally tree-like structure in the infinite size limit. However, only an approximate solution was obtained by use of this method for networks with short loops. Real networks have numerous short and large loops and other complex subgraphs or motifs which lead to essentially non-tree-like neighborhoods. That is why it is important to develop a method which takes into account finite loops and more complex motifs. Different ways were proposed recently to compute loop corrections to the Bethe approximation by use of the belief-propagation algorithm [18, 19]. These methods, however, are exact only if a graph contains a single loop. Loop expansions were proposed in Refs. [20, 21]. However, they were not applied to complex network yet.

Recently, Newman and Miller [22–24] independently introduced a model of random graphs with arbitrary distributions of subgraphs or motifs. In this natural generalization of the configuration model, each vertex belongs to a given set of motifs (e.g., vertex i is a member of $Q^{(1)}(i)$ motifs of type 1, $Q^{(2)}(i)$ motifs of type 2, and so on), and apart of this constraint, the network is uniformly random. In the original configuration model, the sequence of vertex degrees $Q(i)$ is fixed, where $i = 1, 2, ..., N$. In this generalization, the sequence of generalized vertex degrees $Q^{(1)}(i), Q^{(2)}(i), ...$ is given. For example, motifs can be triangles, loops, chains, cliques (fully connected subgraphs), single edges which do not enter other motifs, and, in general, arbitrary finite clusters. The resulting networks can be treated as uncorrelated hypergraphs in which hyperedges represent motifs. In graph theory, a hypergraph is a generalization of a graph, where a hyperedge can connect any number of vertices [25]. Because of the complex motifs, the large sparse networks under consideration can have loops, clustering, and correlations, but the underlying hypergraphs are locally tree-like (hypertrees) and uncorrelated similarly to the original sparse configuration model. Our approach is based on the hypertree-like structure of these highly structured sparse networks. To demonstrate our approach, we apply the generalized belief-propagation algorithm to the fer-

romagnetic Ising model on the sparse networks in which motifs are finite loops or cliques. We obtain an exact solution of the ferromagnetic Ising model and the birth point of the giant connected component in this kind of highly structured networks. Note that the Ising model on these networks is a more complex problem than the percolation problem because we must account for spin interactions between spins both inside and between motifs. We find an exact critical temperature of the ferromagnetic phase transition and demonstrate that finite loops increase the critical temperature in comparison to ordinary tree-like networks.

II. ENSEMBLE OF RANDOM NETWORKS WITH MOTIFS

Let us introduce a statistical ensemble of random networks with a given distribution of motifs in which each vertex belongs to a given set of motifs and apart of this constraint, the networks are uniformly random. These networks can be treated as uncorrelated hypergraphs, in which motifs play a role of hyperedges, so that the number of hyperdegrees are equal to the number of specific motifs attached to a vertex. In principal, one can choose any subgraph with an arbitrary number of vertices as a motif, see Fig. 1. In the present paper, for simplicity, we only consider simple motifs such as single edges, finite loops, and cliques.

Let us first remind how one can describe a statistical ensemble of random networks with the simplest motifs, namely simple edges (see, for example, Refs. [9, 26] and references therein). We define the probability $p_2(a_{ij})$ that an edge between vertices i and j is present ($a_{ij}=1$) or absent ($a_{ij}=0$),

$$p_2(a_{ij}) = \frac{\langle Q_2 \rangle}{N-1}\delta(a_{ij}-1) + \Big(1-\frac{\langle Q_2 \rangle}{N-1}\Big)\delta(a_{ij}) \quad (1)$$

where a_{ij} are entries of the symmetrical adjacency matrix, $\langle Q_2 \rangle = \langle Q \rangle$ is the mean number of edges attached to a vertex. It is well known that the probability of the realization of the Erdős-Rényi graph with a given adjacency matrix a_{ij}, is the product

$$G_2(\{a_{ij}\}) = \prod_{i=1}^{N-1}\prod_{j=i+1}^{N} p_2(a_{ij}). \quad (2)$$

The degree distribution is the Poisson distribution. In the configuration model, the probability of the realization of a given graph with a given sequence of degrees, $Q_2(1)$, $Q_2(2)$, $Q_2(3)$,..., $Q_2(N) \equiv \{Q_2(i)\}$, is

$$G_2(\{a_{ij}\}) = \frac{1}{A}\prod_{i=1}^{N}\delta\Big(Q_2(i) - \sum_{j=1}^{N} a_{ij}\Big)\prod_{i<j} p_2(a_{ij}). \quad (3)$$

The delta-function fixes the number of edges attached to vertex i. A is a normalization constant. The distribution function of degrees is determined by the sequence $\{Q_2(i)\}$,

$$P_2(Q_2) = \frac{1}{N}\sum_i \delta(Q_2 - Q_2(i)). \quad (4)$$

The second simplest motif, triangle, plays the role of a hyperedge which interconnects a triple of vertices. Let us introduce the probability $p_3(a_{ijk})$ that a hyperedge (triangle) between vertices i, j, and k is present or absent, i.e., $a_{ijk}=1$ or $a_{ijk}=0$, respectively:

$$p_3(a_{ijk}) = p\delta(a_{ijk}-1) + (1-p)\delta(a_{ijk}), \quad (5)$$

where

$$p = \frac{2\langle Q_3 \rangle}{(N-1)(N-2)} \quad (6)$$

is the probability that vertices i, j and k form a triangle. $\langle Q_3 \rangle$ is the mean number of triangles attached to a randomly chosen vertex. a_{ijk} are entries of the adjacency matrix of the hypergraph. This matrix is symmetrical with respect to permutations of the indices i, j and k, $a_{ijk} = a_{jki} = a_{kij} = \dots$.

For example, one can introduce the ensemble of the Erdős-Rényi hypergraphs. Given that the matrix elements a_{ijk} are independent and uncorrelated random parameters, the probability of realization of a graph with a given adjacency matrix a_{ijk}, is the product of probabilities $p_3(a_{ijk})$ over different triples of vertices:

$$G_3(\{a_{ijk}\}) = \prod_{i=1}^{N-2}\prod_{j=i+1}^{N-1}\prod_{k=j+1}^{N} p_3(a_{ijk}). \quad (7)$$

This function describes the ensemble of the Erdős-Rényi hypergraphs with the Poisson degree distributions of the number of triangles attached to vertices,

$$P_3(Q_3) = \frac{(\langle Q_3 \rangle)^{Q_3}}{Q_3!}e^{-\langle Q_3 \rangle}. \quad (8)$$

In the configuration model, the probability of the realization of a given graph with a sequence of the number of triangles, $Q_3(1)$, $Q_3(2)$, $Q_3(3)$,...,$Q_3(N) \equiv \{Q_3(i)\}$, attached to vertices $i = 1, 2, \dots, N$ is defined by an equation,

$$G_3(\{a_{ijk}\}) = \frac{1}{A}\prod_{i=1}^{N}\delta\Big(Q_3(i) - \frac{1}{2}\sum_{j,k} a_{ijk}\Big)\prod_{i<j<k} p_3(a_{ijk}). \quad (9)$$

Here $p_3(a_{ijk})$ is given by Eq. (5). The delta-function fixes the number of triangles attached to vertex i. A is a normalization constant. The distribution function of triangles is

$$P_3(Q_3) = \frac{1}{N}\sum_i \delta(Q_3 - Q_3(i)). \quad (10)$$

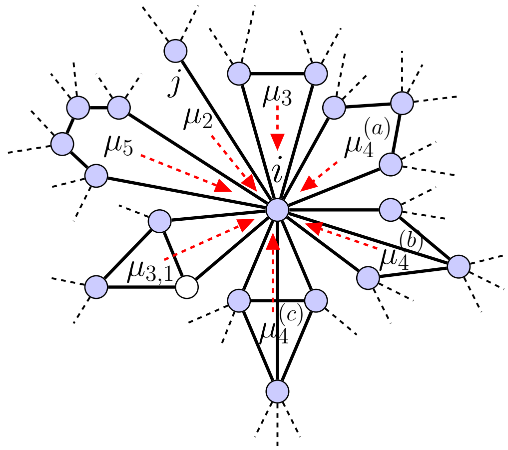

FIG. 1. (Color online) Different motifs can be attached to vertex i in a hypergraph: an ordinary edge a_{ji}, a triangle, a square, and pentagon. There are also non-symmetric motifs consisting of four vertices and the clique of size 4. A motif can have internal vertices (open circle) which have edges only inside this motif. Motifs form a locally tree-like hypergraph where they play a role of hyperedges. Arrows represent incoming messages which arrive at vertex i from the motifs attached to this vertex.

One can further generalize equations Eqs. (5) and (6) and introduce the probability $p_4(a_{ijkl})$ that vertices i, j, k, and l form a hyperedge of size 4 (a clique or loop of size 4). In the case of loops, one can arrange these vertices in order of increasing vertex index. Then, for a given sequence of squares or cliques, $\{Q_4(1), Q_4(2), \dots\}$, attached to vertices $i = 1, 2, \dots$, one can introduce the probability $G_4(\{a_{ijkl}\})$ of the realization of a given graph with a given sequence $\{Q_4(i)\}$ similar to Eq. (9), and so on. The network ensemble of the configuration model with a given sequences of edges $\{Q_2(i)\}$, triangles $\{Q_3(i)\}$, squares $\{Q_4(i)\}$ and other motifs is described by a product of the corresponding probabilities,

$$G(\{a_{ij}\}, \{a_{ijk}\}, \{a_{ijkl}\}, ...) = G_2(\{a_{ij}\}) G_3(\{a_{ijk}\}) ... \tag{11}$$

The average of a quantity $K(\{a_{ij}\}, \{a_{ijk}\}, ...)$ over the network ensemble is

$$\langle K\rangle_{\rm en} = \int K\Big(\{a_{ij}\}, \{a_{ijk}\}, \{a_{ijkl}\}...\Big) \times G(\{a_{ij}\}, \{a_{ijk}\}, \{a_{ijkl}\}, ...) \prod_{i<j} da_{ij} \prod_{i<j<k} da_{ijk} \prod_{i<j<k<l} da_{ijkl} \dots , \tag{12}$$

where we integrate over all possible edges and hyperedges.

One can prove that the probability that different motifs have a common edge, i.e., they are overlapping, tends to zero in the infinite size limit $N \to \infty$. For example, the total number of edges which overlap with triangles equals

$$\left\langle \frac{1}{2} \sum_{i,j,k} a_{ij} a_{ijk} \right\rangle_{\rm en} = \frac{N \langle Q_2\rangle \langle Q_3\rangle}{N-1}. \tag{13}$$

This number of double connections is finite in the limit $N \to \infty$. Because the total number of edges is of the order of N, the fraction of double connections tends to zero in the thermodynamic limit. Thus, one can neglect overlapping between different motifs. Using the standard methods in complex network theory [27–29], one can show that in the configuration model the number of finite loops formed by hyperedges is finite in the thermodynamic limit. Therefore, sparse random uncorrelated hypergraphs have a hypertree-like structure.

Uncorrelated random hypergraphs are described by a distribution function $P(Q_2, Q_3, Q_4, \dots)$ which is the probability that a randomly chosen vertex has Q_2 edges, Q_3 triangles, Q_4 squares, and other motifs attached to this vertex. In the case of uncorrelated motifs, we have

$$P(Q_2, Q_3, Q_4, \dots) = \prod_{\ell=2}^{\infty} P_\ell(Q_\ell). \tag{14}$$

Here, $P_\ell(Q_\ell)$ is the distribution function of loops of size ℓ,

$$P_\ell(Q_\ell) = \frac{1}{N} \sum_i \delta(Q_\ell - Q_\ell(i)). \tag{15}$$

In this kind of network, the number of nearest neighboring vertices of vertex i is equal to

$$Q(i) = Q_2(i) + 2Q_3(i) + 2Q_4(i) + \dots \ . \tag{16}$$

Therefore, the mean degree is

$$\langle Q\rangle = \frac{1}{N} \sum_{i=1}^{N} Q(i) = \sum_{Q_2, Q_3, \dots} Q P(Q_2, Q_3, Q_4, \dots). \tag{17}$$

The local clustering coefficient $C(i)$ of node i with degree $Q(i)$, Eq. (16), is determined by the number of triangles $Q_3(i)$ as follows,

$$C(i) = \frac{2Q_3(i)}{Q(i)(Q(i)-1)}. \tag{18}$$

Therefore, $C(i)$ is maximum if a network only consists of triangles. In this case, we have $Q(i) = 2Q_3(i)$ and therefore

$$C(i) = \frac{1}{Q(i)-1}. \tag{19}$$

On the other hand, if a network only consists of ℓ-cliques with a given ℓ (fully connected subgraphs of size ℓ), then the local clustering coefficient of vertex i with $Q_\ell(i)$ attached cliques equals

$$C(i) = \frac{\ell-2}{Q(i)-1}, \tag{20}$$

where $Q(i) = (\ell - 1)Q_\ell(i)$ is degree of vertex i. If other motifs (edges, squares, and larger finite loops) are present in the network, then according to Eqs. (18) and (20) the local clustering coefficient $C(i)$ is smaller than $(\ell - 2)/(Q(i) - 1)$. In Refs. [30–32], it was shown that properties of networks with "weak clustering", $C(Q) \sim O(1/Q)$, may be different from properties of networks with "strong clustering" when $C(Q)$ decreases slower than $1/Q$. The latter networks are out of the scope of the present paper.

III. BELIEF-PROPAGATION ALGORITHM

Let us consider the Ising model on a sparse random network with arbitrary distributions of motifs. The Hamiltonian of the model is

$$\begin{aligned} E = &- \sum_i H_i S_i - \sum_{i<j} a_{ij} J_{ij} S_i S_j \\ &- \sum_{i<j<k} a_{ijk}(J_{ij}S_iS_j + J_{jk}S_jS_k + J_{ik}S_iS_k) \\ &- \sum_{i<j<k<l} a_{ijkl}(J_{ij}S_iS_j + J_{jk}S_jS_k + J_{kl}S_kS_l + \dots) \\ &+ \dots . \end{aligned} \tag{21}$$

Here we sum energies of spin clusters corresponding to motifs in the network. The second sum corresponds to simple edges. The third sum corresponds to triangles. The forth sum corresponds to motifs of size 4, and so on. The coupling J_{ij} determines the energy of interaction between spins i and j. H_i is a local magnetic field. In general case, the local fields H_i and the couplings J_{ij} can be random quantities.

In order to solve this model, we generalize the belief-propagation algorithm. At first, we remind the belief-propagation algorithm in application for the Ising model on tree-like uncorrelated complex networks without short loops (for more details, see Ref. [9]). In this case, there are only edges determined by the adjacency matrix a_{ij} and clustering coefficient is zero in the thermodynamic limit. Consider spin i. A nearest neighboring spin j sends to spin i a so-called *message* which we denote as $\mu_{ji}(S_i)$. This message is normalized,

$$\sum_{S_i=\pm 1} \mu_{ji}(S_i) = 1. \tag{22}$$

Within the belief-propagation algorithm, the probability that spin i is in a state S_i is determined by the normalized product of incoming messages to spin i and the probabilistic factor $e^{\beta H_i S_i}$ due to a local field H_i:

$$p_i(S_i) = \frac{1}{A} e^{\beta H_i S_i} \prod_j \mu_{ji}(S_i). \tag{23}$$

Here A is a normalization constant, $\beta = 1/T$ is the reciprocal temperature. Now we can calculate the mean moment of spin i,

$$\langle S_i \rangle = \sum_{S_i=\pm 1} S_i p_i(S_i). \tag{24}$$

A message $\mu_{ji}(S_i)$ can be written in a general form,

$$\mu_{ji}(S_i) = \exp(\beta h_{ji} S_i)/[2\cosh(\beta h_{ji})], \tag{25}$$

Using this representation, we rewrite Eq. (24) in a physically clear form,

$$\langle S_i \rangle = \tanh\Big(\beta H_i + \beta \sum_j a_{ji} h_{ji}\Big). \tag{26}$$

This equation shows that a parameter h_{ji} plays a role of an effective field produced by spin j at site i. Messages $\mu_{ji}(S_i)$ obey a self-consistent equation which is called *update rule*,

$$B \sum_{S_j=\pm 1} e^{-\beta E(j,i)} \prod_{n \neq i} \mu_{nj}(S_j) = \mu_{ji}(S_i), \tag{27}$$

where the index n numerates nearest neighbors of vertex j, B is a normalization constant. The diagram representation of this equation is shown in Fig. 2 (a). The probabilistic factor $\exp[-\beta E(j,i)]$ takes account of the interaction energy of spins j and i and a local field H_j,

$$E(j,i) = -H_j S_j - a_{ji} J_{ji} S_i S_j. \tag{28}$$

Thus, a message from j to i is determined by the coupling between these spins and messages received by j from its neighbors except i. Multiplying Eq. (27) by S_i and summing over $S_i = \pm 1$, we obtain a self-consistent equation for the effective fields h_{ji},

$$\tanh(\beta h_{ji}) = \tanh\Big(\beta a_{ji} J_{ji}\Big) \tanh\Big[\beta(H_j + \sum_{n(\neq i)} a_{nj} h_{nj})\Big]. \tag{29}$$

In the thermodynamic limit, this equation is exact for a tree-like graph. The Bethe-Peierls approach and the Baxter recurrence method give exactly the same result [9, 33]. In numerical calculations, equations (27) and (29) may be solved by use of iterations. In a general case, an analytical solution of these equations is unknown. In the case of all-to-all interactions with random couplings J_{ji} (the Sherrington-Kirkpatrick model), this set of equations is reduced to well-known TAP equations [34] which are exact in the thermodynamic limit. These equations also give an exact solution of the ferromagnetic Ising model with uniform couplings $J_{ji} = J > 0$ on a random uncorrelated graph with zero clustering coefficient [9, 35, 36].

Now we generalize the belief-propagation algorithm to the case of networks with given distributions of motifs described in Sec. II. In a network which only consists of edges, a message goes along an edge from the spin at one edge end to the spin at the other edge end. For the networks with motifs, it is natural to introduce a message which is sent by a motif attached to a vertex. This

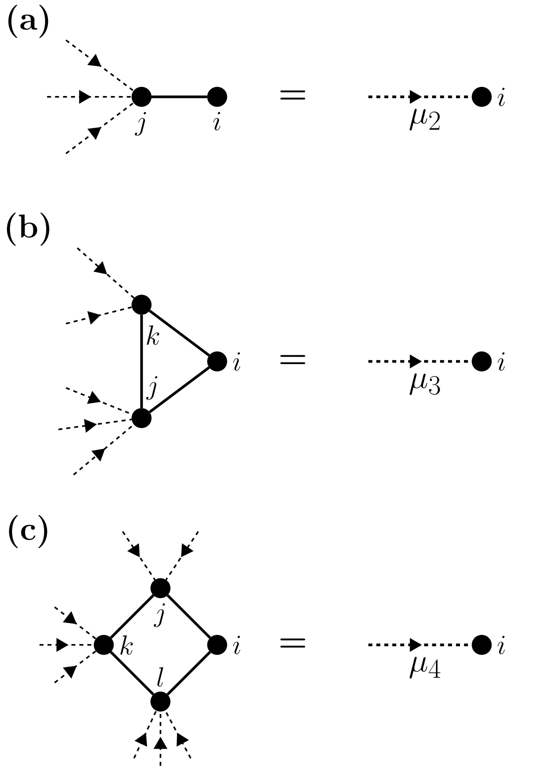

FIG. 2. Diagram representation of the belief-propagation update rules for messages from a motif to a destination vertex i. Arrows represent incoming messages. (a), (b) and (c) represent update rules for an edge, a triangle, and a square. Mathematical expressions of these diagrams are given by Eqs. (27) and (33).

message goes to a spin to which this motif (hyperedge) is attached. Different motifs may be attached to a vertex, see Fig. 1. Let $M_\ell(i)$ denote a cluster of size ℓ attached to vertex i which we will call *destination vertex*. Vertices $j_1, j_2, ..., j_{\ell-1}$ together with the destination vertex i form this motif. We introduce a message $\mu_{M_\ell(i)}(S_i)$ to spin i from a motif $M_\ell(i)$. This message is normalized and can be written as follows,

$$\mu_{M_\ell(i)}(S_i) = \exp\Big(\beta h_{M_\ell(i)} S_i\Big)/[2\cosh(\beta h_{M_\ell(i)})]. \tag{30}$$

As above, the probability that spin i is in a state S_i is determined by the normalized product of incoming messages from motifs attached to spin i and the probabilistic factor $e^{\beta H_i S_i}$,

$$p_i(S_i) = \frac{1}{A} e^{\beta H_i S_i} \prod_{\{M_\ell(i)\}} \mu_{M_\ell(i)}(S_i). \tag{31}$$

Using Eq. (24), we find that the mean moment $\langle S_i \rangle$ is determined by effective fields $h_{M_\ell(i)}$ acting on spin i from motifs $M_\ell(i)$, $\ell = 2, 3, 4, ...$, attached to i, see Fig. 1,

$$\langle S_i \rangle = \tanh\Big(\beta H_i + \beta \sum_{\{M_\ell(i)\}} h_{M_\ell(i)}\Big). \tag{32}$$

Here the sum is taken over motifs attached to i.

Let us find an update rule for a message $\mu_{M_\ell(i)}(S_i)$ from a given motif $M_\ell(i)$ to vertex i. We introduce the following update rule:

$$B \sum_{\{S_j=\pm 1\}} e^{-\beta E(M_\ell(i))} \prod_j \prod_{\{M_n(j) \neq M_\ell(i)\}} \mu_{M_n(j)}(S_j) = \mu_{M_\ell(i)}(S_i). \tag{33}$$

This rule shows that the message $\mu_{M_\ell(i)}(S_i)$ is equal to the product of incoming messages from motifs attached to all spins j in the motif $M_\ell(i)$ except spin i and the motif $M_\ell(i)$ itself (see Fig. 2. In Eq. (33) we average over all spin configurations of the spins $S_{j_1}, S_{j_2}, ...,$ and $S_{j_{\ell-1}}$ in the motif. B is a normalization constant. $E(M_\ell(i))$ is an energy of the interaction between spins in the motif $M_\ell(i)$. This update rule also takes account of local fields H_j acting on all spins except the destination spin i. We would like to note that equation (33) is valid for arbitrary motifs even with a complex internal structure. The only assumption is that a sparse network under consideration, in terms of hypergraphs, has a hypertree-like structure.

For the sake of simplicity, let motifs $M_\ell(i)$ be finite loops of size $\ell = 2, 3, \ldots$ Then

$$E(M_\ell(i)) = -\sum_{n=1}^{\ell-1} H_{j_n} S_{j_n} - \sum_{n=0}^{\ell-1} J_{j_n j_{n+1}} S_{j_n} S_{j_{n+1}}, \tag{34}$$

where $j_0 = j_\ell \equiv i$. If motifs are ℓ-cliques, then the energy $E(M_\ell(i))$ takes account of interactions between all spins in these cliques,

$$E(M_\ell(i)) = -\sum_{j(\neq i)} H_j S_j - \frac{1}{2} \sum_{i,j \in M_\ell(i)} J_{i,j} S_i S_j. \tag{35}$$

Multiplying Eq. (33) by S_i and summing over all spin configurations, we obtain an equation for the effective field $h_{M_\ell(i)}$,

$$\tanh\Big(\beta h_{M_\ell(i)}\Big) = \langle S_i \rangle_{M_\ell(i)}. \tag{36}$$

The function on the right hand side is

$$\langle S_i \rangle_{M_\ell(i)} = \frac{1}{Z(M_\ell(i))} \sum_{\{S_i, S_{j_1}, \ldots = \pm 1\}} S_i e^{-\beta \widetilde{E}(M_\ell(i))}. \tag{37}$$

This function has a meaning of the mean moment of spin S_i in the cluster $M_\ell(i)$ with an energy

$$\widetilde{E}(M_\ell(i)) = -\sum_{n=1}^{\ell-1} H_t(j_n) S_{j_n} - \sum_{n=0}^{\ell} J_{j_n j_{n+1}} S_{j_n} S_{j_{n+1}}. \tag{38}$$

This energy takes into account both the interaction between spins in this motif and total effective fields $H_t(j)$ acting on these spins. In turn, the field $H_t(j)$ acting on j is the sum of a local field H_j and effective fields $h_{M_m(j)}$ produced by incoming messages from motifs $M_m(j)$ attached to vertex j except the motif $M_\ell(i)$, see Fig. 3,

$$H_t(j) = H_j + \sum_{\{M_m(j)(\neq M_\ell(i))\}} h_{M_m(j)}. \tag{39}$$

$Z(M_\ell(i))$ is the partition function of the cluster $M_\ell(i)$,

$$Z(M_\ell(i)) = \sum_{\{S_i, S_{j_1}, \ldots = \pm 1\}} e^{-\beta \widetilde{E}(M_\ell(i))}. \tag{40}$$

Thus, the function $\langle S_i \rangle_{M_\ell(i)}$ is a function $F[H_t(j_1), H_t(j_2), \ldots, H_t(j_{\ell-1})]$ of the total fields $H_t(j)$ acting on all spins in the motif $M_\ell(i)$ except spin i. For a given network with motifs, it is necessary to solve Eq. (36) with respect to the effective fields $h_{M_\ell(i)}$. Then one can calculate the mean magnetic moments $\langle S_i \rangle$ from Eq. (32). Note that the only condition we used to derive the equations above was hypertree-like structure of the networks. The absence of correlations in these hypertree-like networks was not needed. Equations (33) and (36) are our main result which actually generalizes the Bethe-Peierls approach and the Baxter recurrence method.

Let us study the ferromagnetic Ising model with uniform couplings, $J_{ji} = J > 0$, at zero magnetic field, i.e., $H_i = H = 0$, on a uncorrelated hypergraph which consists of edges and finite loops. In a random network, effective fields $h_{M_\ell(i)}$ are also random variable and fluctuate from vertex to vertex. For a given ℓ, we introduce the distribution function of fields $h_{M_\ell(i)}$,

$$\Psi_\ell(h) = \frac{1}{A} \sum_{i=1}^{N} \sum_{\{M_\ell(i)\}} \delta(h - h_{M_\ell(i)}). \tag{41}$$

Here, we sum over vertices i and attached motifs $M_\ell(i)$ of size ℓ. $A = N\langle Q_\ell \rangle$ is the normalization constant. We assume that in the thermodynamic limit, $N \to \infty$, the average over vertices in the network is equivalent to the average over the statistical network ensemble, Eq. (12). Using equation (36), we obtain an equation for the distribution function $\Psi_\ell(h)$,

$$\Psi_\ell(h) = \int \delta\Big(h - T \tanh^{-1}[\langle S \rangle_{M_\ell}]\Big) \prod_{j=1}^{\ell-1} \Phi_\ell(H_t(j)) dH_t(j). \tag{42}$$

Here $\langle S \rangle_{M_\ell}$ is the function $F[H_t(1), H_t(2), \ldots, H_t(\ell-1)]$ defined by Eq. (37). $H_t(j)$ is a total field, Eq. (39), acting on vertex $j = 1, 2, \ldots, \ell-1$ in the motif M_ℓ, see Fig. 3. The integration is over fields $H_t(j)$ with the distribution function $\Phi_\ell(H_t(j))$. Using Eq. (39), we can find this function,

$$\Phi_\ell(H) = \sum_{Q_2, Q_3, \ldots} P(Q_2, Q_3, \ldots) \frac{Q_\ell}{\langle Q_\ell \rangle} \times$$
$$\int \delta\Big(H - \sum_{m(\neq \ell)}^{\infty} \sum_{\alpha=1}^{Q_m} h_{M_m}(\alpha) - \sum_{\alpha=1}^{Q_\ell - 1} h_{M_\ell}(\alpha)\Big) \times$$
$$\prod_{m(\neq\ell)}^{\infty} \Big(\prod_{\alpha=1}^{Q_m} \Psi_m(h_{M_m}(\alpha)) dh_{M_m}(\alpha) \Big) \prod_{\alpha=1}^{Q_\ell - 1} \Psi_\ell(h_{M_\ell}(\alpha)) dh_{M_\ell}(\alpha). \tag{43}$$

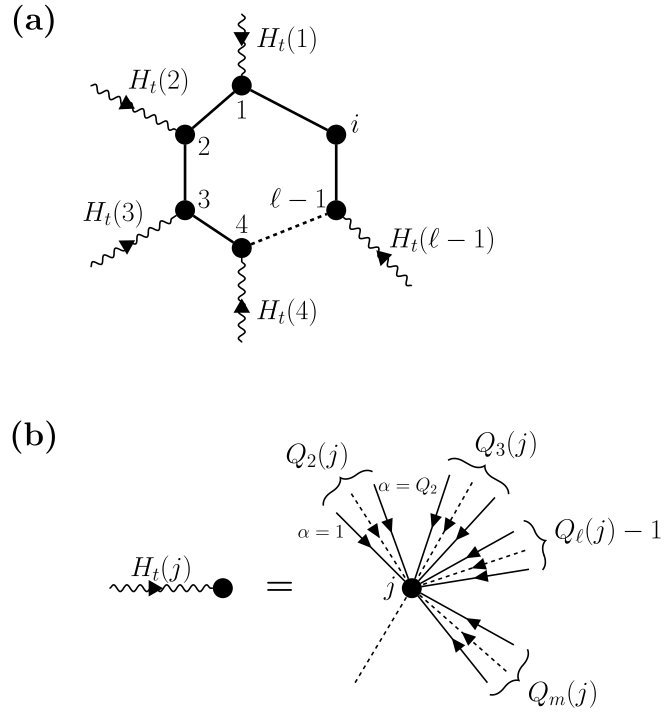

FIG. 3. (a) A loop (motif M_ℓ) of size ℓ is attached to destination vertex i. Wave arrows represent total effective fields $H_t(j)$ acting on spins with index $j = 1, 2, \ldots, \ell-1$ in this loop. (b) In turn, the total effective field $H_t(j)$ is a sum of effective fields produced by all motifs attached to vertex j except the motif M_ℓ. There are $Q_2(j)$ edges, $Q_3(j)$ triangles, and so on. However, the number of loops of size ℓ equals $Q_\ell(j) - 1$, because we should not account the motif M_ℓ which is common for vertices j and i.

Here $P(Q_2, Q_3, ...)$ is given by Eq. (14). This is the probability that a destination vertex has Q_2 edges, Q_3 triangles, and so on. In turn, incoming messages $h_{M_m}(\alpha)$ to the destination spin from attached loops of size m are numerated by the index α, $\alpha = 1, 2, ..., Q_m$. Only for incoming messages from loops of size ℓ we have $\alpha = 1, 2, ..., Q_\ell - 1$, because we should not account for the motif M_ℓ. The integration is over incoming messages to all vertices in the motif (hyperedge) M_ℓ except the destination vertex i, see Fig. 3. Note that we have an additional factor $Q_\ell / \langle Q_\ell \rangle$, because in the configuration model $P_\ell(Q_\ell) Q_\ell / \langle Q_\ell \rangle$ is the probability that if we arrive at a destination vertex along a hyperedge M_ℓ, then this vertex has $Q_\ell - 1$ outgoing hyperedges M_ℓ. Equations (42) and (43) represent a set of self-consistent equations for the functions $\Psi_\ell(h)$, $\ell = 2, 3, 4, \ldots$. Then, using Eq. (32), one can find a distribution function of spontaneous magnetic moments $\langle S_i \rangle$ in the network. Equations (42) and (43) are also valid for networks with cliques.

IV. CRITICAL TEMPERATURE

In the paramagnetic phase at zero magnetic field, there is no spontaneous magnetization and the effective fields are equal to zero, i.e., $h_{M_\ell} = 0$. Therefore, we obtain

$$\Psi_\ell(h) = \delta(h). \tag{44}$$

for any ℓ. This is the only solution of Eqs. (42) and (43) in the paramagnetic phase. Below a critical temperature T_c, this solution becomes unstable and a non-trivial solution for the function $\Psi_\ell(h)$ emerges. In this case, a mean value of the effective field h_{M_ℓ},

$$\langle h_{M_\ell} \rangle_T = \int h \Psi_\ell(h) dh, \tag{45}$$

becomes non-zero. Here $\langle ... \rangle_T$ means the thermodynamic average. In the case of a continuous phase transition, $\langle h_{M_\ell} \rangle_T$ tends to zero if temperature T tends to T_c from below. Let use this fact. From Eq. (36) we obtain

$$\int \tanh(\beta h) \Psi_\ell(h) dh = \int \langle S \rangle_{M_\ell} \prod_{j=1}^{\ell-1} \Phi_\ell(H_t(j)) dH_t(j). \tag{46}$$

We expand the functions $\tanh(\beta h)$ and $\langle S \rangle_{M_\ell}$ on the left and right hand sides of this equation in small h and $H_t(j)$, respectively:

$$\tanh(\beta h) = \beta h + O(h^3),$$
$$\langle S_i \rangle_{M_\ell} = \sum_{j=1}^{\ell-1} \chi_\ell(ij) H_t(j) + O(H_t^3(j)), \tag{47}$$

where we define

$$\chi_\ell(ij) \equiv \frac{\partial \langle S_i \rangle_{M_\ell}}{\partial H_t(j)}\Big|_{H_t(j)=0} = \beta \langle S_i S_j \rangle_{M_\ell}\Big|_{H_t(j)=0}. \tag{48}$$

$\chi_\ell(ij)$ is a non-local susceptibility in a spin cluster M_ℓ at zero magnetic field. Note that $T\chi_\ell(ii) = 1$. Assuming that at $T \to T_c - 0$ the first moment of the function $\Psi_\ell(h)$, i.e., $\langle h_{M_m} \rangle_T$, is much larger than higher moments, i.e., $\langle h_{M_m} \rangle_T \gg \langle h^n_{M_m} \rangle_T$, in the leading order we obtain a linear equation,

$$\langle h_{M_\ell} \rangle_T = \frac{F_\ell(T)}{\langle Q_\ell \rangle} \Big[\langle Q_\ell (Q_\ell - 1) \rangle \langle h_{M_\ell} \rangle_T + \sum_{m(\neq \ell)}^{\infty} \langle Q_\ell Q_m \rangle \langle h_{M_m} \rangle_T \Big], \tag{49}$$

where $\langle \dots \rangle$ defines an average over the distribution function $P(Q_2, Q_3, Q_4, \dots)$ given by Eq. (14). The function $F_\ell(T)$ is defined as follows,

$$F_\ell(T) \equiv T \sum_{j=1}^{\ell-1} \chi_\ell(ij) = T\chi_\ell - 1, \tag{50}$$

χ_ℓ is the total zero-field magnetic susceptibility of the Ising model on a ring of size ℓ. Simple calculations give

$$F_2(T) = t, \qquad \ell = 2,$$
$$F_\ell(T) = \frac{2t(1 - t^{\ell-1})}{(1-t)(1+t^\ell)}, \qquad \ell \geq 3, \tag{51}$$

where $t = \tanh(J/T)$. In the paramagnetic phase, the set of linear equations (49) for parameters $\langle h_{M_\ell} \rangle_T$ only has a trivial solution, $\langle h_{M_\ell} \rangle_T = 0$. A non-trivial solution appears at a temperature at which

$$det \widehat{M} = 0, \tag{52}$$

where the matrix M_{mn} is defined as follows:

$$M_{mn} = \langle Q_m Q_n \rangle, \qquad m \neq n,$$
$$M_{mm} = \langle Q_m (Q_m - 1) \rangle - \frac{\langle Q_m \rangle}{F_m(T)}, \tag{53}$$

for $m, n = 2, 3, \dots$. Equation (52) determines the critical point T_c of the continuous phase transition. Below T_c, spontaneous effective fields appear, i.e., $\langle h_{M_\ell} \rangle_T \neq 0$. Therefore, there is a non-zero spontaneous magnetic moment. If all motifs are loops of equal length ℓ, then the critical temperature T_c is determined by the equation

$$B_\ell F_\ell(T) = 1 \tag{54}$$

where B_ℓ is the average branching coefficient for these hyperedges (ℓ-loops in this network),

$$B_\ell = \frac{\langle Q_\ell (Q_\ell - 1) \rangle}{\langle Q_\ell \rangle}. \tag{55}$$

In particular, if there are only edges, i.e., $\ell = 2$, then Eq. (54) gives

$$T_c = 2J / \ln\Big(\frac{B_2 + 1}{B_2 - 1} \Big). \tag{56}$$

This result was found for uncorrelated random complex networks with arbitrary degree distributions [9, 35, 36]. Figure 4 shows the dependence of the critical temperature T_c versus the mean number of nearest neighbors $\langle Q \rangle = 2\langle Q_\ell \rangle$, Eq. (17), in the networks having ℓ-loop motifs, in which the Poissonian distribution of hyperdegrees is assumed. In this case $B_\ell = Q_\ell$. One can see that, at a given $\langle Q \rangle$, the larger the loops the larger the critical temperature. At $\ell = 2$ (an ordinary Erdős-Rényi graph), the Ising model has a lower T_c in comparison to that at $\ell = 3$. In the limit $\langle Q \rangle = 2\langle Q_\ell \rangle \gg 1$, we find that

$$T_c(\ell = 2)/J \cong 2\langle Q_\ell \rangle + o(1),$$
$$T_c(\ell \geq 3)/J \cong 2\langle Q_\ell \rangle + 1 + o(1), \tag{57}$$

If there are only two motifs, for example, loops of size ℓ and ℓ', then Eq. (52) leads to the equation

$$\Big[B_\ell - \frac{1}{F_\ell(T)} \Big] \Big[B_{\ell'} - \frac{1}{F_{\ell'}(T)} \Big] = \frac{\langle Q_\ell Q_{\ell'} \rangle^2}{\langle Q_\ell \rangle \langle Q_{\ell'} \rangle}. \tag{58}$$

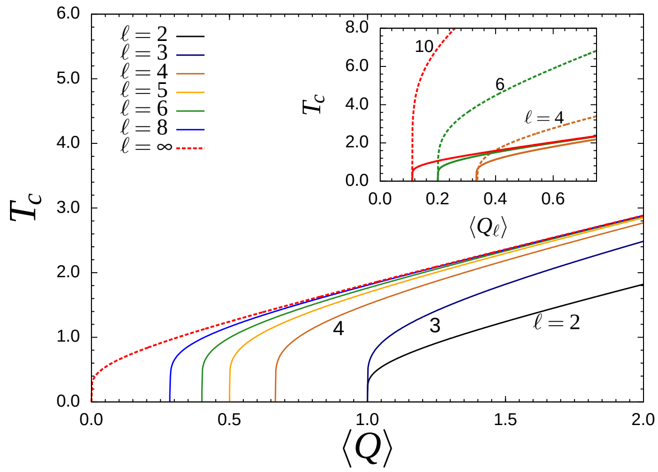

FIG. 4. (Color online) Critical temperature T_c of the ferromagnetic Ising model versus the mean number of nearest neighbors $\langle Q \rangle = 2\langle Q_\ell \rangle$ in uncorrelated random networks with Poisson distribution of loops of size ℓ and the mean number $\langle Q_\ell \rangle$ of these loops attached to a vertex. Note that the case $\ell = 2$ is special: there are no loops, and we have the Erdős-Rényi graph. Inset displays T_c versus the mean number $\langle Q_\ell \rangle$ of ℓ-cliques (dashed lines), and, for comparison, T_c for finite loops of the same size ℓ (solid lines). Here we put $J = 1$.

From Eqs. (51) and (54), it follows that if an uncorrelated random hypergraph has a divergent second moment $\langle Q_m^2 \rangle$ for any $m \geq 2$, then T_c becomes infinite in the infinite size limit. This result was obtained for ordinary uncorrelated random complex network in Refs. [9, 35, 36]. Moreover, because equations (42) and (43) have analytical properties similar to ones studied in Refs. [9, 35, 36], we conclude that the ferromagnetic Ising model on considered loopy networks has the same critical properties as ones on ordinary uncorrelated random networks.

Another example of complex motifs are ℓ-cliques. Calculating the susceptibility χ of a cluster of spins on this subgraph, we can find the function $F_\ell(T)$ from Eq. (50) at $\ell \geq 3$,

$$F_\ell(T) = (\ell - 1)\Big[1 - \frac{4I_{\ell-2}(T)}{I_\ell(T)}\Big]. \tag{59}$$

Here we introduced the function

$$I_\ell(T) = \sum_{n=0}^{\ell} C_n^\ell \exp\Big[\frac{1}{2}\beta J(2n-\ell)^2\Big], \tag{60}$$

where $C_n^\ell = n!/(n-\ell)!\ell!$ is the binomial coefficient. If a network only consists of uncorrelated ℓ-cliques then the critical temperature of the ferromagnetic Ising model is given by Eq. (54) with the function Eq. (59). In the case of the Poisson distribution of ℓ-cliques with the mean degree $\langle Q_\ell \rangle \gg 1$, we obtain an asymptotic result,

$$T_c \approx (\ell - 1)\langle Q_\ell \rangle. \tag{61}$$

It is not wonder that this critical temperature is larger than T_c, Eq. (57), of a network consisting of short loops of size ℓ at a given mean degree $\langle Q_\ell \rangle$. This result shows that the internal structure of motifs may influence strongly critical properties of the Ising model although that the percolation threshold may be the same (see below).

V. PERCOLATION THRESHOLD

Equation (52) permits us to find the percolation threshold in these loopy networks. Below the percolation threshold, a network consists of finite clusters and there is no giant component. In this case, there is no phase transition in the Ising model. This spin system is in a paramagnetic state at any T. At a point of the birth of a giant component, there is a giant connected cluster and the critical temperature is $T_c = 0$. Above the percolation threshold, the critical temperature is non-zero, $T_c > 0$. Therefore, in a general case for an arbitrary distribution function $P(Q_2, Q_3, Q_4, ...)$, the percolation point is determined by Eq. (52) at $T = 0$. In this case, we have $F_\ell(T = 0) = \ell - 1$. For example, if there are only loops of size ℓ and ℓ' then Eq. (58) takes a form,

$$\Big[B_\ell - \frac{1}{\ell - 1}\Big]\Big[B_{\ell'} - \frac{1}{\ell' - 1}\Big] = \frac{\langle Q_\ell Q_{\ell'} \rangle^2}{\langle Q_\ell \rangle \langle Q_{\ell'} \rangle}. \tag{62}$$

In the case of ℓ-loop motifs, equation (54) gives the following criterion for the birth of a giant connected component:

$$(\ell - 1)B_\ell = 1, \tag{63}$$

where B_ℓ is the average branching. At $\ell = 2$, this is the Molloy-Reed criterion for ordinary uncorrelated random networks [37]. The percolation threshold can be seen in Fig. 4 as a critical value of the mean degree $\langle Q \rangle$, Eq. (17), below which T_c is zero. Our results about the percolation threshold agree with results obtained in Refs. [22, 24, 38] by use of different approaches. It is interesting that we have $F_\ell(T = 0) = \ell - 1$ for both finite loops and cliques of the same size ℓ. Therefore, the percolation threshold Eq. (63), i.e., the point of birth of the giant component, is also the same.

VI. CONCLUSION

In the present paper, we considered highly structured sparse networks with arbitrary distributions of motifs, which locally have hypertree-like structure. Using the configuration model for hypergraphs, we introduced a statistical ensemble of these random networks and found the probability of the realization of the network with a given sequence of edges, finite loops, and cliques. We generalized the belief-propagation algorithm to networks with arbitrary distributions of motifs. Using this algorithm, we solved the Ising model on the networks with arbitrary distributions of finite loops and cliques. We found

an exact critical temperature of the ferromagnetic Ising model with uniform coupling between spins. We demonstrated that clustering increases the critical temperature in comparison with an ordinary tree-like network with the same mean degree. We showed that networks with loops of large size have a larger critical temperature in comparison with networks having loops of smaller size. Our solution also enabled us to find the birth point of the giant connected component in sparse networks with arbitrary distributions of finite loops and cliques in agreement with Refs. [22, 24, 38]. We believe that the proposed generalized belief propagation algorithm may be used for studying dynamical processes and variety of models on highly structured networks with complex motifs.

ACKNOWLEDGMENTS

This work was partially supported by the following projects PTDC: FIS/71551/2006, FIS/108476/2008, SAU-NEU/103904/2008, and MAT/114515/2009. S. Y. was supported by FCT under Grant No. SFRH/BPD/38437/2007.

[1] J. Pearl, *Probabilistic Reasoning in Intelligent Systems: Networks of Plausible Inference* (Morgan Kaufmann, San Francisco, 1988).
[2] B. J. Frey, *Graphical models for machine learning and digital communication* (MIT Press, Cambridge, 1998).
[3] R. J. McEliece, D. J. C. MacKay, and J. F. Cheng, IEEE J. Select. Areas Commun. **16**, 140 (1998).
[4] J. S. Yedidia, W. T. Freeman, and Y. Weiss, in *Advances in Neural Information Processing Systems*, edited by T. K. Leen, T. G. Dietterich, and V. Tresp, pp. 689-695 (MA: MIT Press, Cambridge, 2001).
[5] M. Pretti and A. Pelizzola, J. Phys. A **36**, 11201 (2003).
[6] J. M. Mooij and H. J. Kappen, J. Stat. Mech. P11012 (2005).
[7] A. K. Hartmann and M. Weigt, *Phase Transitions in Combinatorial Optimization Problems: Basics, Algorithms and Statistical Mechanics* (Wiley-VCH, 2005).
[8] M. Mézard and G. Parisi, J. Stat. Phys.**111**, 1 (2003).
[9] S. N. Dorogovtsev, A. V. Goltsev, and J. F. F. Mendes, Rev. Mod. Phys. **80**, 1275 (2008).
[10] J. M. Mooij and H. J. Kappen, *Advances in Neural Information Processing Systems* (MIT Press, Cambridge, 2005), Vol.17, pp. 945-952.; eprint arXiv:cond-mat/0408378v2 (2004).
[11] J. Ohkubo, M. Yasuda, and K. Tanaka, Phys. Rev. E **72**, 046135 (2005).
[12] B. Karrer and M. E. J.Newman, Phys. Rev. E **82**, 016101 (2010).
[13] Y. Shiraki and Y. Kabashima, Phys. Rev. E **82**, 036101 (2010).
[14] G. Bianconi and N. Gulbahce, J. Phys. A: Math. Theor. **41**, 224008 (2008).
[15] P. Šulc and L. Zdeborová, J. Phys. A: Math. Theor. **43**, 285003 (2010).
[16] J. Reichardt, R. Alamino, and D. Saad, eprint arXiv:1012.4524v1 (2010).
[17] A. Steimer, W. Maass, and R. Douglas, Neural Computation **21**, 2502 (2009).
[18] A. Montanari and T. Rizzo, J. Stat. Mech. P10011 (2005).
[19] G. Parisi and F. Slanina, J. Stat. Mech. L02003 (2006).
[20] M. Chertkov and V. Y. Chernyak, J. Stat. Mech., P06009 (2006).
[21] M. Chertkov and V. Y. Chernyak, Phys. Rev. E **73**, 065102 (2006).
[22] M. E. J. Newman, Phys. Rev. Lett. **103**, 058701 (2009).
[23] J. C. Miller, Phys. Rev. E **80**, 020901(R) (2009).
[24] B. Karrer and M. E. J. Newman, Phys. Rev. E **82**, 066118 (2010).
[25] C. Berge, *Graphs and Hypergraphs* (North-Holland, Amsterdam, 1973)
[26] G. Bianconi, Phys. Rev. E **79**, 036114 (2009).
[27] G. Bianconi and A. Capocci(2003), Phys. Rev. Lett. **90**, 078701 (2003).
[28] G. Bianconi and M. Marsili, J. Stat. Mech., P06005 (2005).
[29] M. E. J. Newman, Phys. Rev. E **68**, 026121 (2003).
[30] M. A. Serrano and M. Boguna, Phys. Rev. Lett. **97**, 088701 (2006).
[31] M. A. Serrano and M. Boguna, Phys. Rev. E **74**, 056114 (2006).
[32] M. A. Serrano and M. Boguna, Phys. Rev. E **74**, 056115 (2006).
[33] R.J. Baxter, *Exactly Solved Models in Statistical Mechanics* (Academic Press, London, 1982).
[34] D. J. Thouless, P. W. Anderson, and R. G. Palmer, Philos. Mag. **35**, 593 (1977).
[35] S. N. Dorogovtsev, A. V. Goltsev and J. F. F. Mendes, Phys. Rev. E **66**, 016104 (2002).
[36] M. Leone, A. Vázquez, A. Vespignani, and R. Zecchina, Eur. Phys. J. B **28**, 191 (2002).
[37] M. Molloy and B. A. Reed, Random Struct. Algor. **6**, 161 (1995).
[38] A. Hackett, S. Melnik, and J. P. Gleeson, eprint arXiv:1012.3651 (2011).